IUST Iran University of Science and Technology

Iranian Journal of Electrical and Electronic Engineering

Journal Homepage: ijeee.iust.ac.ir

Neuro-Second Order Sliding Mode Control of a DFIG Supplied by a Two-Level NSVM Inverter for Wind Turbine System

H. Benbouhenni*(C.A.), Z. Boudjema** and A. Belaidi*

Abstract: This paper applied second order sliding mode control (SOSMC) strategy using artificial neural network (ANN) on the rotor side converter of a 1.5 MW doubly fed induction generator (DFIG) integrated in a wind turbine system. In this work, the converter is controlled by a neural space vector modulation (NSVM) technique in order to reduce powers ripples and total harmonic distortion (THD) of stator current. The validity of the proposed control technique applied on the DFIG is verified by Matlab/Simulink. The active power, reactive power, torque and stator current are determined and compared with conventional control method. Simulation results presented in this paper shown that the proposed control scheme reduces the THD value and powers ripples compared to traditional control under various operating conditions.

Keywords: Doubly Fed Induction Generator, Artificial Neural Network, Space Vector Modulation, Neural Space Vector Modulation, Total Harmonic Distortion, Second Order Sliding Mode Control.

1 Introduction

WIND energy is becoming one of the most important renewable power sources used nowadays. Recently, power converter command has mostly been studied and developed for wind power conversion system (WECS) integration in the electrical grid. The use of energy electronic converters allows variable speed operation of the WECS to extracts maximum power from the turbine [1].

The DFIG has been widely used for large scale wind generation systems [2]. However, the stator winding directly connected to the grid and the rotor winding connected to the grid through a variable frequency converter. On the other hand, various control methods has been proposed in the literature, for studying the behavior of the DFIG based wind conversion system during normal operation. The most important are: vector control (VC) [3-5], direct torque control (DTC) [6-8], direct power control (DPC) [9-11], intelligent control (IC) [12, 13], robust control (RC) [14, 15], backstepping control (BC) [16]. In literature [17], VC command is the most popular technique used in the DFIG based wind energy conversion system. However, this control scheme gives more powers ripples and big THD of stator current.

For robust and high performance VC command, a sliding mode controller (SMC) was studied in the literature [18-20]. However, the SMC technique was proposed by Utkin in 1977 [21]. This control method based on the theory of variable structure systems has been extensively employed for nonlinear systems [22]. Like every control techniques have some advantages and disadvantages, SMC control has too. Some of the advantages are presented in [23]. The basic disadvantages of the SMC method using sat or sign function are the chattering phenomenon. Many papers have been proposed to overcome this problem. In [24], second order sliding mode controller was designed to command the active and reactive powers. SMC and fuzzy controller are combined to command the

Iranian Journal of Electrical and Electronic Engineering, 2018.
Paper first received 27 February 2018 and accepted 12 May 2018.
* The authors are with the Ecole Nationale Polytechnique d'Oran Maurice Audin, Algeria.
E-mails: habib0264@gmail.com and belaidiaek@gmail.com.
** The author is with the Electrical Engineering Department, Faculty of Technology, Hassiba Benbouali University, Chlef, Algeria.
E-mail: boudjemaa1983@yahoo.fr.
Corresponding Author: H. Benbouhenni.

DFIG [25]. In [26], a hybrid control based on fuzzy logic controller and a second order sliding mode was designed to command the DFIG based WECS. In this paper, we propose a new second order sliding mode control (SOSMC) based on ANN. However, in the aim to augment the performances of the DFIG control we propose in this paper a hybrid method based on SOSMC and ANN, the results control scheme is known as (NSOSMC).

Traditionally, the space vector modulation (SVM) technique is widely used for control of multilevel inverters of AC machines. The principle of SVM method is detailed in [27-29]. On the other hand, this technique gives minimum THD and powers ripples compared with pulse width modulation (PWM) technique. In this work, we propose a new SVM technique based on ANN controller named (NSVM). This technique gives more and more minimum of THD value, simple scheme and easy to implement compared with conventional SVM method.

In this paper, we apply the NSOSMC technique on the DFIG based wind power conversion system using NSVM strategy compared to the conventional SVM inverter.

2 NSVM Technique

In this section, we propose an SVM technique based on ANN controller. However, the ANN consists of several cascaded layers of neurons with sigmoid activation functions [30]. On the other hand, The ANN controller has many models. The ANN controller contains three layers: output layers, hidden layers, and input layers. Each layer is composed of several neurons [31].

Since SVM method based on the principles of space vectors and need to calculate of sector and angle [32, 33]. On the other hand, we propose a new SVM technique of two-level inverter based on calculation of maximum and minimum of three-phase voltages (V_a, V_b, V_c). The advantages of the proposed SVM method is not needed to calculate the sector and angle, easy to implement and gives a strong performance for the real-time feedback command compared with PWM technique. Fig. 1 shows the principle of the SVM technique of two-level inverter.

The principle of the NSVM is similar to traditional SVM. However, the hysteresis controllers are replaced by neural controllers and this method based on neural classification has the advantage of simplicity and easy implementation. On the other hand, the NSVM gives more and more minimum THD of stator current compared to traditional SVM technique. The structure of SVM based on ANN controller is shown in Fig. 2.

The convergence of the network in summer obtained by using the value of the parameters grouped in Table 1. The structure of the ANN controller used to perform the SVM technique is an ANN with one linear input node, 12 neurons in the hidden layer, and one neuron in the output layer. As shown in Fig. 3 the ANN controller is composed of two layers, Layer 1 (Fig. 4) and Layer 2 (Fig. 5).

3 Model of Turbine

The wind turbine input energy usually is:

$$P_v = 0.5\rho S_w V_w^3 \tag{1}$$

The output mechanical power of wind turbine is:

$$P_m = C_p P_v = 0.5\rho C_p S_w V_w^3 \tag{2}$$

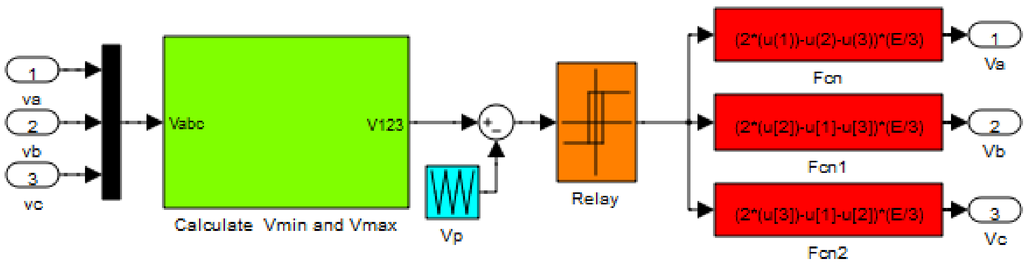

Fig. 1 Simulation block of proposed SVM technique.

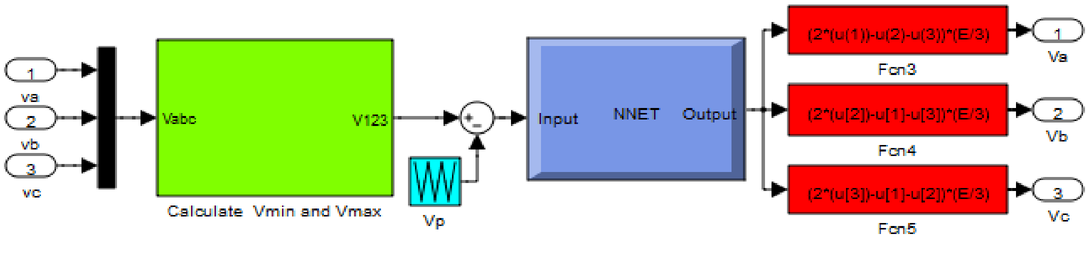

Fig. 2 SVM method with ANN controller.

Table 1 Parameters of the LM for hysteresis controllers.

Parameters of the LM	Values
Number of hidden layer	12
TrainParam.Lr	0.002
TrainParam.show	50
TrainParam.eposh	1000
Coeff of acceleration of convergence (mc)	0.9
TrainParam.goal	0
TrainParam.mu	0.9
Functions of activation	Tensing, Purling, gensim

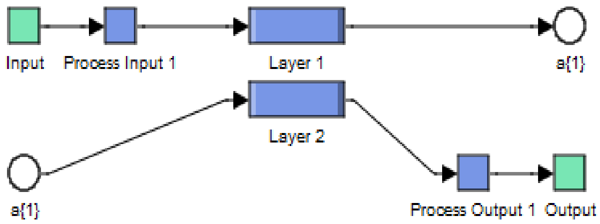

Fig. 3 Structure of ANN hysteresis comparators.

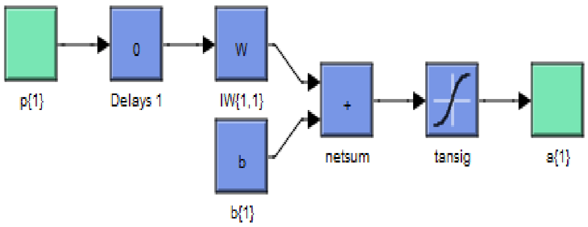

Fig. 4 Layer 1.

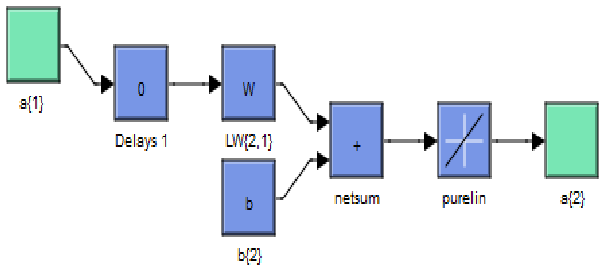

Fig. 5 Layer 2.

The ration of the tip speed of the turbine blades to wind speed is:

$$\lambda = \frac{R\Omega t}{v} \tag{3}$$

C_p can be described as [34, 35]:

$$C_p(\beta,\lambda) = C_1\left(\frac{C_2}{\lambda_i} - C_3\beta - C_4\right)\exp\left(\frac{-C_5}{\lambda_i}\right) + C_6\lambda \tag{4}$$

$$\frac{1}{\lambda_i} = \frac{1}{\lambda + 0.08\beta} - \frac{0.035}{\beta^3 + 1} \tag{5}$$

The torque produced by the turbine is expressed in the following way:

$$T_t = \frac{P_t}{\Omega_t} = 0.5\rho\pi R^3 V_w^2 C_t \tag{6}$$

$$C_t = \frac{C_p}{\lambda} \tag{7}$$

where: C_p represents the wind turbine power conversion efficiency. ρ is air density, S_w is wind turbine blades swept area in the wind, V is wind speed. R is blade radius. **Ω** is angular speed of the turbine. C_t is the torque coefficient. $C1 = 0.5176$, $C2 = 116$, $C3 = 0.4$, $C4 = 5$, $C5 = 21$, $C6 = 0.0068$.

4 Model of DFIG

The traditional electrical equations of the DFIG in the Park frame are written as follows [36, 37]:

$$\begin{cases} V_{ds} = R_s I_{ds} + \frac{d}{dt}\psi_{ds} - \omega_s \psi_{qs} \\ V_{qs} = R_s I_{qs} + \frac{d}{dt}\psi_{qs} + \omega_s \psi_{ds} \\ V_{dr} = R_r I_{dr} + \frac{d}{dt}\psi_{dr} - \omega_r \psi_{qr} \\ V_{qr} = R_r I_{qr} + \frac{d}{dt}\psi_{qr} + \omega_r \psi_{dr} \end{cases} \tag{8}$$

The rotor and stator flux can be expressed as:

$$\begin{cases} \psi_{ds} = L_s I_{ds} + M I_{dr} \\ \psi_{qs} = L_s I_{qs} + M I_{qr} \\ \psi_{dr} = L_r I_{dr} + M I_{ds} \\ \psi_{qr} = L_r I_{qr} + M I_{qs} \end{cases} \tag{9}$$

The reactive and active powers at the stator can be expressed as:

$$\begin{cases} P_s = \frac{3}{2}\left(V_{ds} I_{ds} + V_{qs} I_{qs}\right) \\ Q_s = \frac{3}{2}\left(V_{qs} I_{ds} - V_{ds} I_{qs}\right) \end{cases} \tag{10}$$

The electromagnetic torque is expressed as:

$$T_e = pM\left(I_{dr} I_{qs} - I_{qr} I_{ds}\right) \tag{11}$$

$$T_e = T_r + J\frac{d\Omega}{dt} + f\,\Omega \tag{12}$$

where V_{dr}, V_{qr}, V_{qs} and V_{ds}, are the two-phase rotor and stator voltages, I_{dr}, I_{qr}, I_{ds} and I_{qs}, are the two-phase rotor and stator currents, ψ_{dr}, ψ_{qr}, ψ_{ds} and ψ_{qs}, are the two-phase rotor and stator fluxes, L_r, L_s and M are respectively the inductance own rotor, stator, and the mutual inductance between two coils, R_r and R_s are respectively the resistances of the stator and rotor windings,.ω_s is the electrical pulsation of the stator and ω_r is the rotor one. T_r is the load torque, T_e is the electromagnetic torque, Ω is the mechanical rotor speed, J is the inertia, f is the viscous friction coefficient and p is the number of pole pairs. P_s is the stator active power, Q_s is the stator reactive power.

5 Robust Control Strategies of DFIG

In this section, comparison of DFIG performances using two nonlinear controllers: second order sliding mode, neuro-second order sliding mode.

5.1 Second Order Sliding Mode Control

Sliding mode control is an effective robust control technique for unmatched perturbations [38]. The principle of this technique is detailed in [39]. The major disadvantage of the SMC controller is the chattering phenomenon. To eliminate the chattering phenomenon, a second order sliding mode is proposed in [40, 41], and widely applied to various systems [42-44]. In [45], second order sliding mode controller is developed to control DFIM machine. In [46], second order sliding mode control is developped to control reactive and active powers of DFIG.

The second order sliding mode control (SOSMC) does not need accurate mathematical models like classical controllers. On the other hand, we choose the error between the reference stator energies and measured as second order sliding mode surfaces, so we can write the following expression:

$$\begin{bmatrix} S_p \\ S_q \end{bmatrix} = \begin{bmatrix} P_{sref} - P_s \\ Q_{sref} - Q_s \end{bmatrix} \tag{13}$$

We derived the above errors, we obtain

$$\begin{bmatrix} \dot{S}_p \\ \dot{S}_q \end{bmatrix} = \begin{bmatrix} \dot{P}_{sref} - P_s \\ \dot{Q}_{sref} - Q_s \end{bmatrix} \tag{14}$$

Then we will have

$$\begin{bmatrix} \dot{S}_p \\ \dot{S}_q \end{bmatrix} = \begin{bmatrix} \dot{P}_{sref} - \dfrac{\alpha}{\sigma L_r}\left(V_{qr} - R_r I_{qr} - g w_s \sigma L_r I_{dr} - g\dfrac{M V_s}{L_s}\right) \\ \dot{Q}_{sref} - \dfrac{\alpha}{\sigma L_r}\left(V_{dr} - R_r I_{dr} + g w_s \sigma L_r I_{qr}\right) \end{bmatrix} \tag{15}$$

where $\alpha = -V_s M / L_s$. If we define the A_1 and A_2 functions as follows.

$$\begin{bmatrix} A_1 \\ A_2 \end{bmatrix} = \begin{bmatrix} \dot{P}_{sref} - \dfrac{\alpha}{\sigma L_r}\left(-R_r I_{qr} - g w_s \sigma L_r I_{dr} - g\dfrac{M V_s}{L_s}\right) \\ \dot{Q}_{sref} - \dfrac{\alpha}{\sigma L_r}\left(-R_r I_{dr} - g w_s \sigma L_r I_{qr}\right) \end{bmatrix} \tag{16}$$

Thus we have

$$\begin{bmatrix} \dot{S}_p \\ \dot{S}_q \end{bmatrix} = \begin{bmatrix} \dfrac{\alpha}{\sigma L_r} V_{qr} + A_1 \\ \dfrac{\alpha}{\sigma L_r} V_{dr} + A_2 \end{bmatrix} \tag{17}$$

On deriving the relationship of Eq. (17) yields:

$$\begin{bmatrix} \ddot{S}_p \\ \ddot{S}_q \end{bmatrix} = \begin{bmatrix} \dfrac{\alpha}{\sigma L_r} \dot{V}_{qr} + \dot{A}_1 \\ \dfrac{\alpha}{\sigma L_r} \dot{V}_{dr} + \dot{A}_2 \end{bmatrix} \tag{18}$$

The SOSMC proposed based on the super twisting algorithm known (ST) which is introduced by Levant.

$$V_{dr} = u_1 + u_2 \tag{19}$$

Then it follows that

$$\begin{bmatrix} u_1 \\ u_2 \end{bmatrix} = \begin{bmatrix} -\lambda_1 \operatorname{sgn}(S_q) \\ -\delta_1 |S_q|^{0.5} \operatorname{sgn}(S_q) \end{bmatrix} \tag{20}$$

And

$$V_{qr} = w_1 + w_2 \tag{21}$$

Including

$$\begin{bmatrix} w_1 \\ w_2 \end{bmatrix} = \begin{bmatrix} -\lambda_2 \operatorname{sgn}(S_p) \\ -\delta_2 |S_p|^{0.5} \operatorname{sgn}(S_p) \end{bmatrix} \tag{22}$$

To ensure the convergence of regulators in the infinity of time constants and are chosen to satisfy the following inequality

$$\begin{cases} \lambda_i \le \dfrac{\mu_i}{\sigma L_r} \\ \delta_i \ge \dfrac{4\mu_i(\lambda_i + \mu_i)}{(\lambda_i - \mu_i)(L_r \sigma)^2} \\ |A_i| \prec \mu_i \quad \forall i = 1, 2 \end{cases} \tag{23}$$

Fig. 6 shows the block diagram of second order sliding mode control strategy.

5.2 Neuro-Second Order Sliding Mode Control

The application of artificial neural networks attracts the attention of many scientists from all over the world [47]. This intelligent technique have many advantages, it is simple architecture, inexact input data, the possibility of approximating non-linear function, insensitivity to the distortion of the network, easy of training and generalization [48]. The neuro-second order sliding mode control (NSOSMC) is similar to a traditional SOSMC. However, the switching controller term sign ($S(x)$), has been replaced by ANN controller as given by Fig. 7. On the other hand, the NSOSMC give more and more minimum powers ripples compared with traditional SOSMC method.

The structure of the proposed neural controllers was a network with one linear input node, 8 neurons in the hidden layer, and one neuron in the output layers.

Fig. 8 shows the neural network training performance of ANN controllers for active and reactive powers. Fig. 9 shows the internal structure of ANN controller for active and reactive powers. Fig. 10 shows the block diagram of the internal structure of hidden layer.

6 Simulation Results

In this section, simulations are carried out with a 1.5MW DFIG machine attached to a 398V/50Hz grid, using the Matlab/Simulink. Parameters of the DFIG are given in Table. 2. Two control strategies, SOSMC-SVM and NSOSMC-NSVM, are simulated and compared regarding reference tracking, powers ripples, stator current harmonics distortion, and robustness against DFIG parameter variations.

6.1 Reference Tracking Test

Figs. 11-12 shows the harmonic spectrums of one phase stator current of the DFIG obtained using Fast Fourier Transform (FFT) method for SOSMC-SVM and NSOSMC-NSVM one respectively. Table 3 shows the comparative analysis of THD value. It can be clear observed that the THD is reduced for NSOSMC-NSVM control method (THD = 0.16%) when compared to SOSMC-SVM (THD = 0.40%).

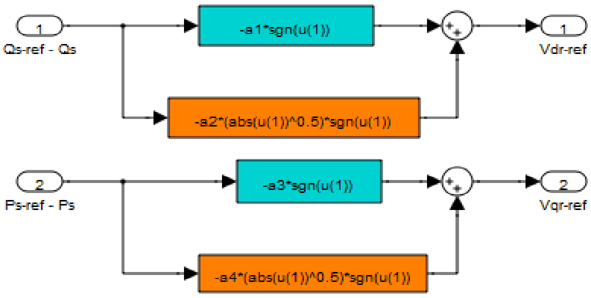

Fig. 6 Block diagram of SOSMC method.

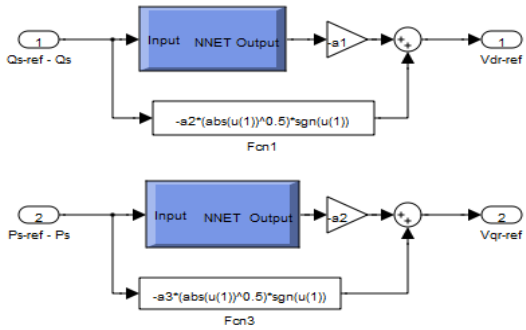

Fig. 7 Block diagram of NSOSMC strategy.

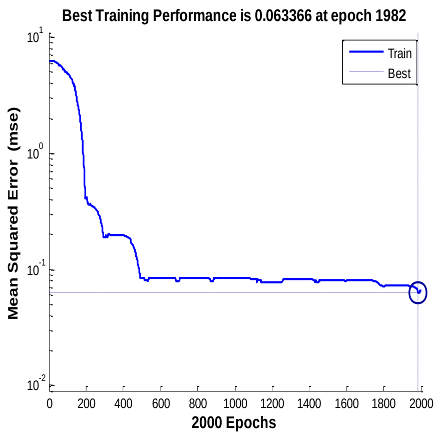

Fig. 8 Neural network training performance.

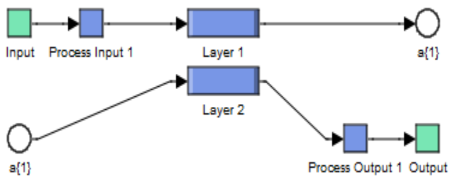

Fig. 9 The internal structure of ANN controllers.

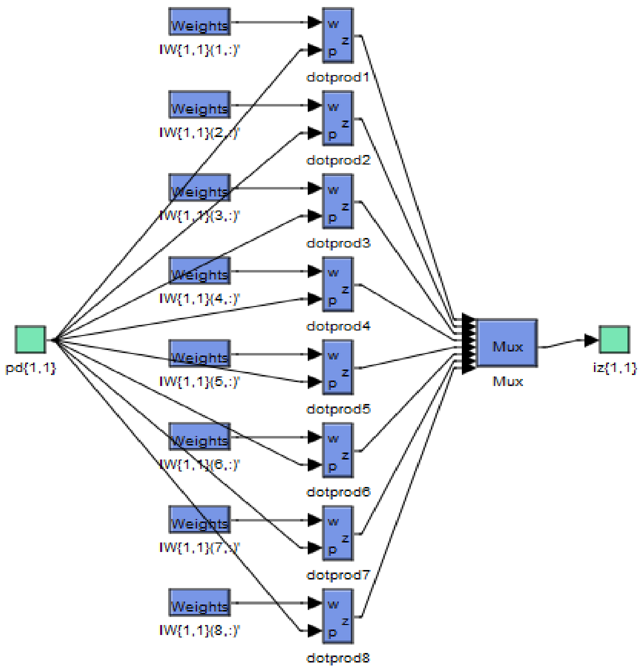

Fig. 10 Block diagram of the internal structure of hidden layer.

Figs. 13-15 show the obtained simulation results. For the proposed command strategies, the stator reactive and active power tracks almost perfectly their references values. Moreover, the NSOSMC-NSVM control strategy reduced the powers ripples and torque ripple compared to the SOSMC-SVM control scheme (See Figs. 16-18).

Table 2 The DFIG parameters.

Parameters	Rated Value	Unity
Nominal power	1.5	MW
Stator voltage	398/690	V
Stator frequency	50	Hz
Number of pairs poles	2	
Stator resistance	0.012	Ω
Rotor resistance	0.021	Ω
Stator inductance	0.0137	H
Rotor inductance	0.0136	H
Mutual inductance	0.0135	H
Inertia	1000	$Kg.m^2$
Viscous friction	0.0024	Nm/s

Table 3 Comparative analysis of THD value (tracking test).

	THD (%)	
	SOSMC-SVM	NSOSMC-NSVM
Stator current	0.40	0.16

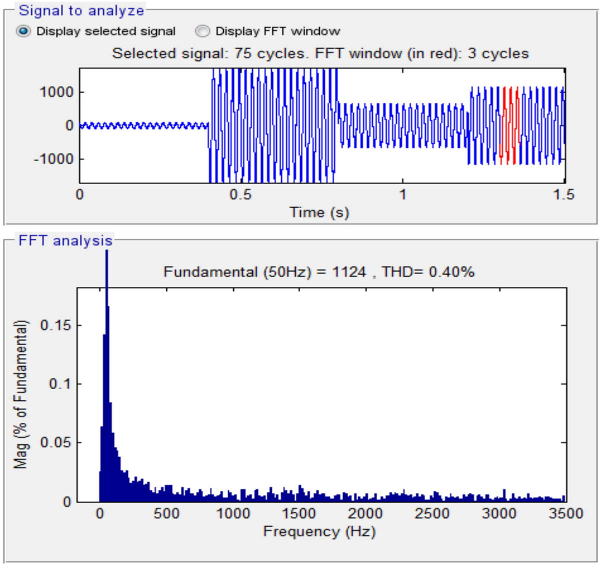

Fig. 11 THD of one phase stator current for SOSMC-SVM control (reference tracking test).

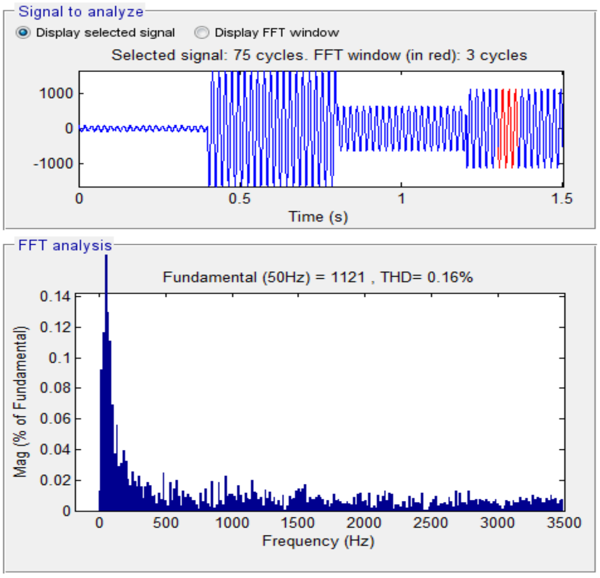

Fig. 12 THD of one phase stator current for NSOSMC-NSVM control (reference tracking test).

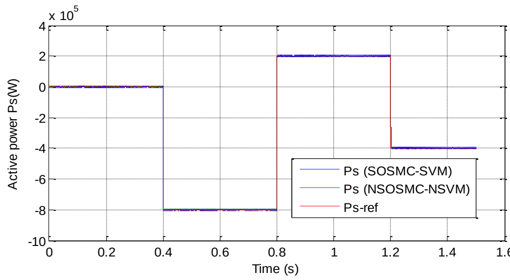

Fig. 13 Active power (reference tracking test).

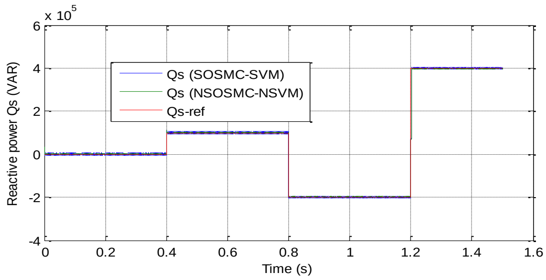

Fig. 14 Reactive power (reference tracking test).

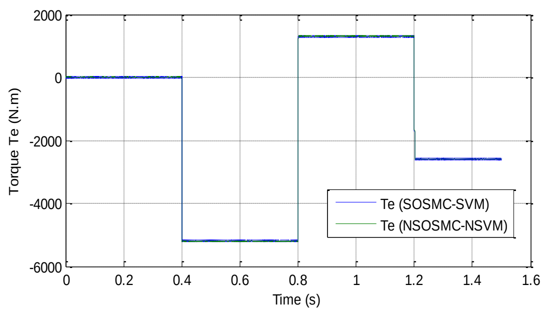

Fig. 15 Torque (reference tracking test).

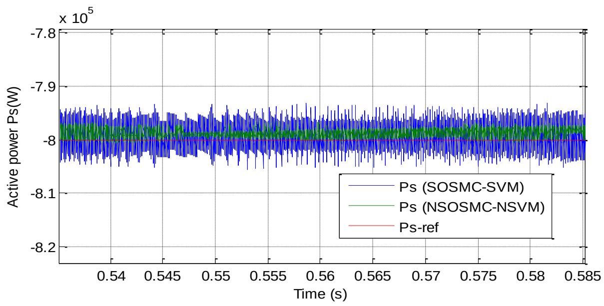

Fig. 16 Zoom in the active power (reference tracking test).

6.2 Robustness Test

In order to examine the robustness of the proposed controls schemes, the nominal value of the R_r and R_s is multiplied by 2, the values of inductances L_s, M, and L_r are multiplied by 0.5. Simulation results are presented in Figs. 19-23. As it is shown by these Figures, these variations present a clear effect on the active, reactive powers, and electromagnetic torque curves and that the effect appears more important for the SOSMC-SVM control scheme compared to NSOSMC-NSVM control (see Figs. 24-26). On the other hand, the THD value of stator current in the NSOSMC-NSVM has been reduced significantly. Table 4 shows the comparative analysis of THD value. Thus it can be concluded that the NSOSMC-NSVM control scheme is more robust than the SOSMC-SVM control.

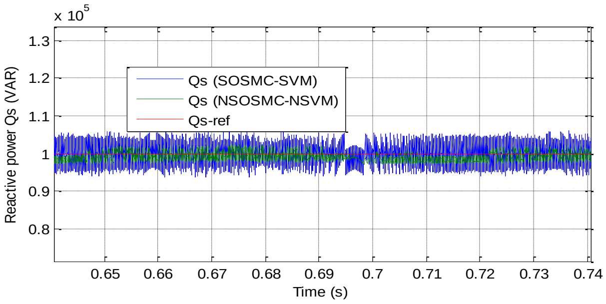

Fig. 17 Zoom in the reactive power (reference tracking test).

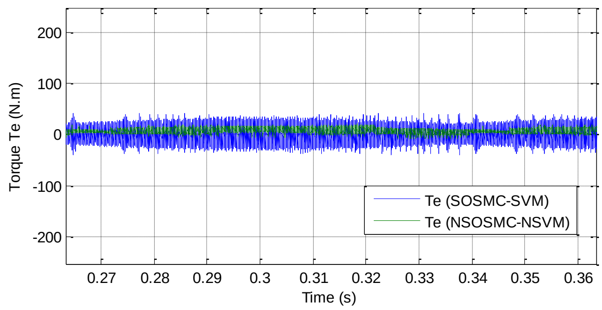

Fig. 18 Zoom in the torque (reference tracking test).

Table 4 Comparative analysis of THD value (robustness test).

	THD (%)	
	SOSMC-SVM	NSOSMC-NSVM
Stator current	0.84	0.31

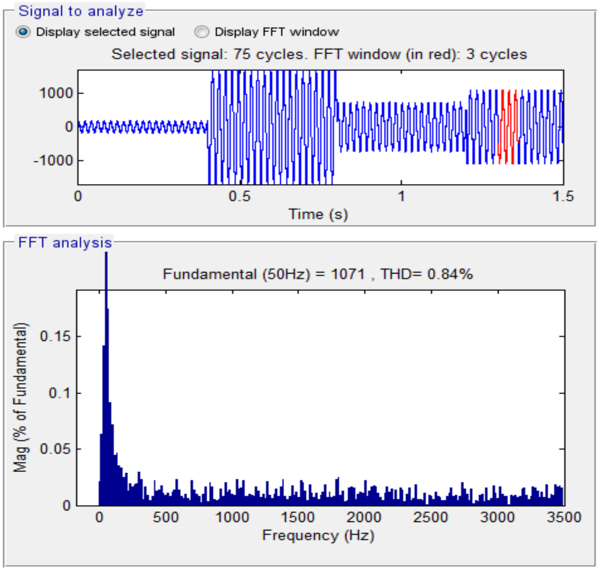

Fig. 19 THD of one phase stator current for SOSMC-SVM control (robustness test).

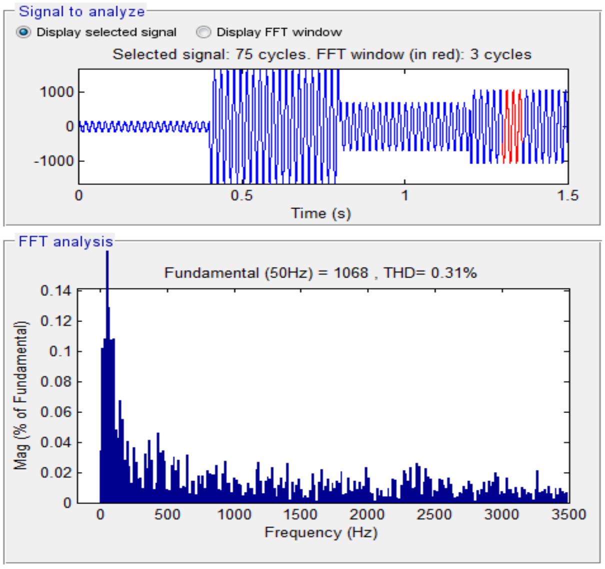

Fig. 20 THD of one phase stator current for NSOSMC-NSVM (robustness test).

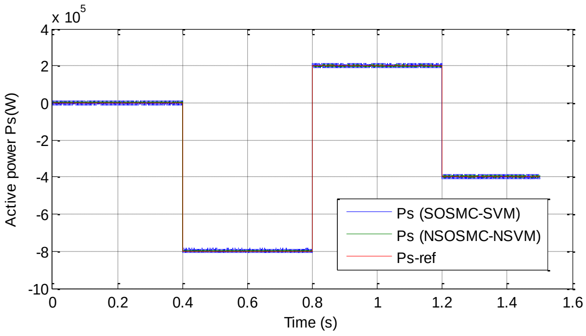

Fig. 21 Active power (robustness test).

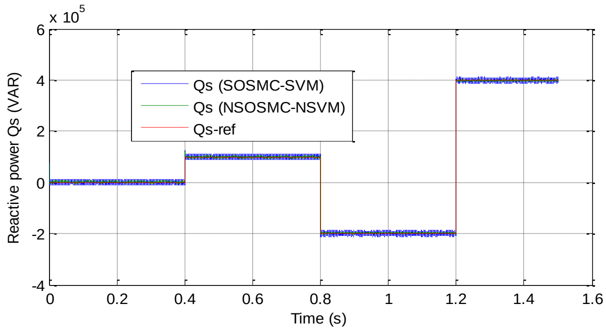

Fig. 22 Reactive power (robustness test).

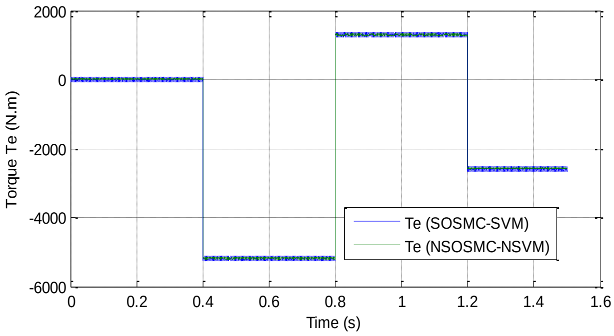

Fig. 23 Torque (robustness test).

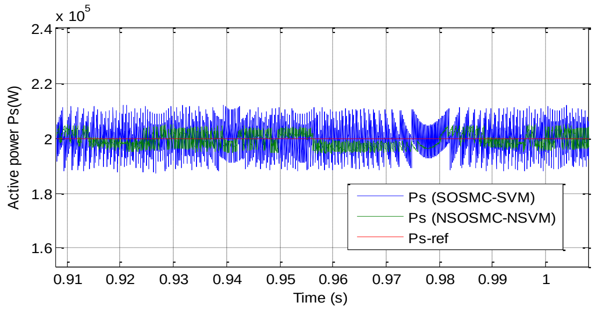

Fig. 24 Zoom in the active power (robustness test).

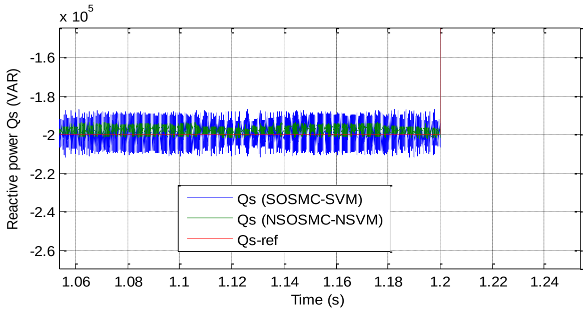

Fig. 25 Zoom in the reactive power (robustness test).

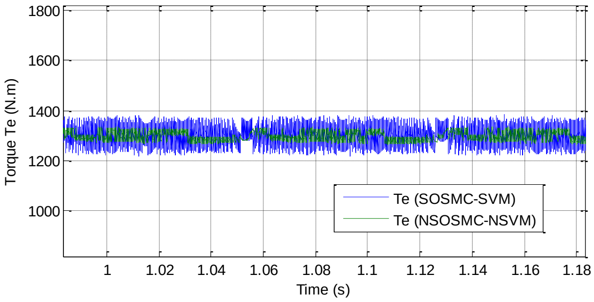

Fig. 26 Zoom in the torque (robustness test).

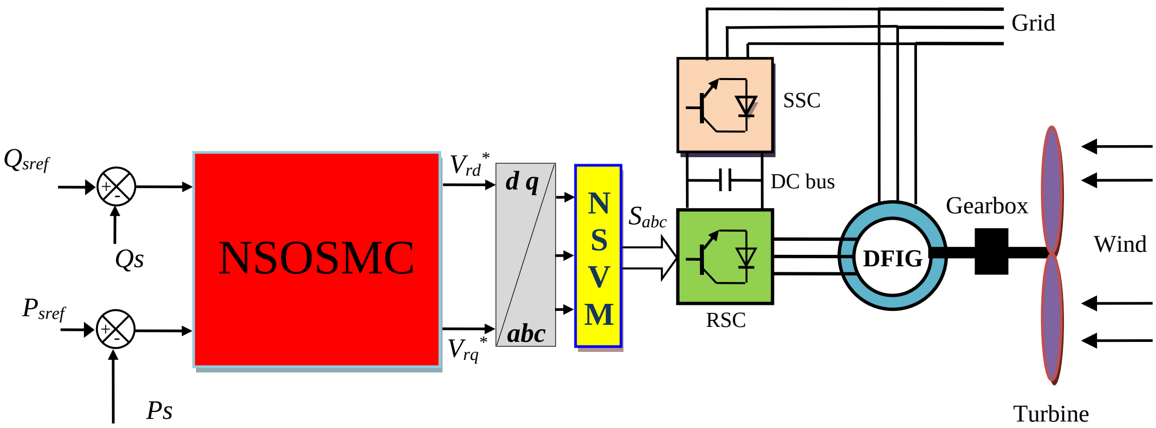

Fig. 27 Block diagram of NSOSMC-NSVM control.

7 Conclusion

The simulation and the control of a WECS based on a DFIG connected directly to the grid by the stator and fed by a two-level converter on the rotor side has been presented in this article. Our objective was the implementation of a NSOSMC technique of stator reactive and active powers generated by the stator side of the DFIG in order to make the system insensible with the external disturbance and the parametric variation. On the other hand, we proposed a NSVM technique to control the two-level inverter. This new modulation gives a minimum THD value and powers ripples compared with conventional modulation technique. However, the various results obtained in simulation show the proposed command (NSOSMC-NSVM) robustness to the system and load parameters disturbances. The results obtained with this control are very interesting compared to the conventional SOSMC-SVM control in eliminating of the active and reactive powers ripples, chattering phenomenon and THD value of stator current. The NSOSMC-NSVM control has the advantage of being easily implemented by a program command and simple scheme.

Appendix

A. NSOSMC Control Block with NSVM Inverter

The NSOSMC control of a DFIG based on NSVM inverter is shown in Fig. 27.

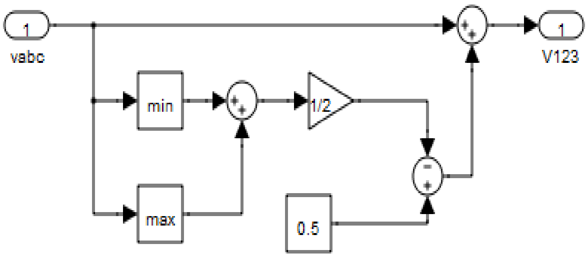

Fig. 28 Block diagram of SVM strategy.

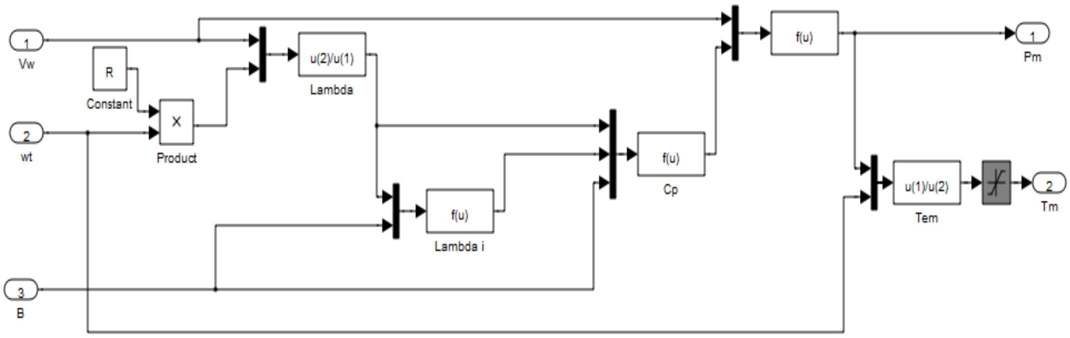

Fig. 29 Block diagram of wind turbine.

B. Block Diagram of SVM Inverter

The proposed SVM technique of a DFIG based wind turbine system is shown in Fig. 28.

C. Block Diagram of Wind Turbine

The block diagram of wind turbine system is shown in Fig. 29.

The proposed SVM technique based on following steps:

1) Calculates the minimum voltages (min (V_a, V_b, V_c)).
2) Calculates the maximum voltages (max (V_a, V_b, V_c)).
3) Add the maximum and minimum voltages (max (V_a, V_b, V_c) + min (V_a, V_b, V_c)).
4) The last step is to compare step-3 waveforms with V_p ($V_{Triangle}$), and generates the pulses for that switch presents in the three phase voltage source converter circuit.

References

[1] Y. Bekakra and D. B. Attous, "DFIG sliding mode control driven by wind turbine with using a SVM inverter for improve the quality of energy injected into the electrical grid," *ECTI Transactions on Electrical Engineering, Electronics, and Communications*, Vol. 11, No. 1, pp. 63–75, 2013.

[2] E. G. Shehata, "Sliding mode direct power control of RSC for DFIGs driven by variable speed wind turbines," *Alexandria Engineering Journal*, Vol. 54, pp. 1067–1075, 2015.

[3] A. Medjber, A. Moualdia, A. Mellit and M. A. Guessoum, "Comparative study between direct and indirect vector control applied to a wind turbine equipped with a double-fed asynchronous machine article," *International Journal of Renewable Energy Research*, Vol. 3, No. 1, pp. 88–93, 2013.

[4] K. Kerrouche, A. Mezouar and Kh. Belkacem, "Decoupled control of doubly fed induction generator by vector control for wind energy conversion system," *Energy Procedia*, Vol. 42, pp. 239–248, 2013.

[5] F. Amrane, A. Chaiba, B. Babas and S. Mekhilef, "Design and implementation of high performance field oriented control for grid-connected doubly fed induction generator via hysteresis rotor current controller," *Revue Roumaine des Sciences Techniques Serie Electrotechnique et Energetique*, Vol. 61, No. 4, pp. 319–324, 2016.

[6] Z. Boudjema, R. Taleb, Y. Djerriri and A. Yahdou, "A novel direct torque control using second order continuous sliding mode of a doubly fed induction generator for a wind energy conversion system," *Turkish Journal of Electrical Engineering & Computer Sciences*, Vol. 25, pp. 965–975, 2017.

[7] Y. Wa and W. Yang, "Different control strategies on the rotor side converter in DFIG-based wind turbines," *Energy Procedia*, Vol. 100, pp. 551–555, 2016.

[8] Y. S. Rao and A. J. Laxmi, "Direct torque control of doubly fed induction generator based wind turbine under voltage dips," *International Journal of Advances in Engineering & Technology*, Vol. 3, pp. 711–720, 2012.

[9] S. Massoum, A. Meroufel, A. Massoum and P. Wira, "A direct power control of the doubly-fed induction generator based on the SVM strategy," *Elektrotehniski Vestnik*, Vol. 45, No. 5, pp. 235–240, 2017.

[10] S. M. Tavakoli, M. A. Pourmina and M. R. Zolghadri, "Comparison between different DPC methods applied to DFIG wind turbines," *International Journal of Renewable Energy Research*, Vol. 3, No. 2, pp. 446–452, 2013.

[11] A. Izanlo, S. A. Gholamian and M. V. Kazemi, "Comparative study between two sensorless methods for direct power control of doubly fed induction generator," *Revue Roumaine des Sciences Techniques Serie Electrotechnique et Energetique*, Vol. 62, No. 4, pp. 358-364, 2017.

[12] A. Bakouri, H. Mahmoudi and A. Abbou, "Intelligent control for doubly fed induction generator connected to the electrical network," *International Journal of Power Electronics and Drive System*, Vol. 7, No. 3, pp. 688–700, 2016.

[13] M. M. Ismail and A. F. Bendary, " Protection of DFIG wind turbine using fuzzy logic control," *Alexandria Engineering Journal*, Vol. 55, pp. 941–949, 2016.

[14] Z. Boudjema, A. Meroufel, and A. Amari, "Robust control of a doubly fed induction generator (DFIG) fed by a direct AC-AC converter," *Przegląd Elektrotechniczny*, Vol. 11, pp. 213–221, 2012.

[15] O. Barambones and J. M. Gonzalez de Durana, "Sliding mode control for power output maximization in a wave energy systems," *Energy Procedia*, Vol. 75, pp. 265–270, 2015.

[16] M. El-Azzaoui, H. Mahmoudi, K. Boudaria, "Backstepping control of wind and photovoltaic hybrid renewable energy system," *Internationale Journal of Power Electronics and Drive Systems*, Vol. 7, No. 3, pp. 677–686, 2016.

[17] F. Amrane and A. Chaiba, "A novel direct power control for grid-connected doubly fed induction generator based on hybrid artificial intelligent control with space vector modulation," *Revue Roumaine des Sciences Techniques Serie Electrotechnique et Energetique*, Vol. 61, No. 3, pp. 263–268, 2016.

[18] A. Etxeberria, I. Vechiu, H. Camblong and J. M. Vinassa, "Comparison of sliding mode and PI control of a hybrid energy storage system in a microgrid application," *Energy Procedia*, Vol. 12, pp. 966–974, 2011.

[19] A. Allaoua and A. Laoufi, "A novel sliding mode fuzzy control based on SVM for electric vehicles propulsion system," *Energy Procedia*, Vol. 36, pp. 120–129, 2013.

[20] M. S. Merzoug, H. Benalla and L. Louze, "Sliding mode control (SMC) of permanent magnet synchronous generators (PMSG)," *Energy Procedia*, Vol. 18, pp. 43–52, 2012.

[21] Y. Bekakra and D. Ben Attous, "Comparison study between SVM and PWM inverter in sliding mode control of active and reactive power control of a DFIG for variable speed wind energy," *International Journal of Renewable Energy Research*, Vol. 2, No. 3, pp. 471–476, 2012.

[22] Z. Boudjema, R. Taleb, and A. Yahdou, "A new DTC scheme using second order sliding mode and fuzzy logic of a DFIG for wind turbine system," *International Journal of Advanced Computer Science and Applications*, Vol. 7, No. 8, pp. 49–56, 2016.

[23] M. Benkahla, R. Taleb and Z. Boudjema, "Comparative study of robust control strategies for a DFIG-based wind turbine," *International Journal of Advanced Computer Science and Applications*, Vol. 7, No. 2, pp. 455–462, 2016.

[24] A. Yahdou, B. Hemici and Z. Boudjema, "Second order sliding mode control of a dual-rotor wind turbine system by employing a matrix converter," *Journal of Electrical Engineering*, Vol. 16, No. 4, pp. 1–11, 2016.

[25] S. E. Ardjoun and M. Abid, "Fuzzy sliding mode control applied to a doubly fed induction generator for wind turbines," *Turkish Journal of Electrical Engineering & Computer Sciences*, Vol. 23, pp. 1673–1686, 2015.

[26] F. Z. Tria, K. Srairi, M. T. Benchouia, B. Mahdad and M. E. Benbouzid, "An hybrid control based on fuzzy logic and a second order sliding mode for MPPT in wind energy conversion systems," *International Journal on Electrical Engineering and Informatics*, Vol. 8, No. 4, pp. 711–726, 2016.

[27] D. Kanimozhi, S. Saravanan and R. Satheeshkumar, "Analysis of doubly fed induction generator connected matrix converter in wind farm," *International Journal of Engineering Research & Technology*, Vol. 2, pp. 3981–3988, 2013.

[28] F. Bishwang, T. Guanzheng and F. Shaosheng, "Comparison of three different 2-D space vector PWM algorithms and their FPGA implementations," *Journal of Power Technologies*, Vol. 94, No. 3, pp. 176–189, 2014.

[29] M. Gaballah, M. El-Bardini, S. Sharaf and M. Mabrouk, "Implementation of space vector-PWM for driving two level voltage source inverters," *Journal of Engineering Sciences*, Vol. 39, No. 4, pp. 871–884, 2011.

[30] A. Moosavienia and K. Mohammadi, "A generalized ABFT technique using a fault tolerant neural network," *Iranian Journal of Electrical & Electronic Engineering*, Vol. 1, No. 1, pp. 1–10, 2005.

[31] E. Benyoussef, A. Meroufel and S. Barakat, "Three-level DTC based on fuzzy logic and neural network of sensorless DSSM using extende kalman filter," *International Journal of Power Electronics and Drive System*, Vol. 5, No. 4, pp. 453–463, 2015.

[32] H. Obdan and M. C. Ozkilic, "Performance comparison of 2-level and 3-level converters in a wind energy conversion system," *Revue Roumaine des Sciences Techniques Serie Electrotechnique et Energetique*, Vol. 61, No. 4, pp. 388–393, 2016.

[33] E. E. M. Mohamed and M. A. Sayed, "Matrix converters and three-phase inverters fed linear induction motor drives-performance compare," *Ain Shams Engineering Journal*, Vol. 2, pp. 1–12, 2016.

[34] Z. Boudjema, A. Meroufel, Y. Djerriri and E. Bounadja, "Fuzzy sliding mode control of a doubly fed induction generator for wind energy conversion," *Carpathian Journal of Electronic and Computer Engineering*, Vol. 6, No. 2, pp. 7–14, 2013.

[35] N. Khemiri, A. Khedher and M. F. Mimouni, "Wind energy conversion system using DFIG controlled by backstepping and sliding mode strategies," *International Journal of Renewable Energy Research*, Vol. 2, No. 3, 2012, pp. 422–435.

[36] M. Hasni, Z. Mancer, S. Mekhtoub and S. Bacha, "Parametric identification of the doubly fed induction machine," *Energy Procedia*, Vol. 18, pp. 177–186, 2012.

[37] E. Bounadja, A. Djahbar and Z. Boudjema, "Variable structure control of a doubly fed induction generator for wind energy conversion systems," *Energy Procedia*, Vol. 50, pp. 999–1007, 2014.

[38] H. Moradi and V. J. Majd, "A dissipative integral sliding mode control redesign method for uncertain nonlinear switched systems," *Iranian Journal of Electrical and Electronic Engineering*, Vol. 11, No. 4, pp. 310–318, 2015.

[39] M. Adjoudj, M. Abid, A. Aissaoui, Y. Ramdani and H. Bounoua, "Sliding mode control of a doubly fed induction generator for wind turbines," *Revue Roumaine des Sciences Techniques Serie Electrotechnique et Energetique*, Vol. 56, No. 1, pp. 15–24, 2011.

[40] Y. B. Shtessel, I. A. Shkolnikov and M. D. Brown, "An asymptotic second-order smooth sliding mode control," *Asian Journal of Control*, Vol. 5, No. 4, pp. 498–504, 2003.

[41] A. Pisano, "Second order sliding modes: theory and applications," *Phd Thesis, Dipartimento di Ingegneria Elettrica ed Elettronica, univerista Degli Studi di, Cagliari*, 2000.

[42] R. Hendel, F. Khaber and N. Essounbouli, "Adaptive type-2 fuzzy second order sliding mode control for nonlinear uncertain chaotic system," *International Journal of Computational Science, Information Technology and Control Engineering*, Vol. 2, No. 4, pp. 1–14, 2015.

[43] B. Beltran, M. E. H. Benbouzid and T. Ahmed-Ali, "Second-order sliding mode power control and grid fault-tolerance of a DFIG-based wind turbine," *Revue Roumaine des Sciences Techniques Serie Electrotechnique et Energetique*, Vol. 2, No. 1, pp. 75–91, 2011.

[44] D. Kim, K. Koo, J. J. Jeong, T. Goh and S. W. Kim, "Second-order siscrete-time sliding mode observer for state of charge determination based on a dynamic resistance Li-Ion battery model," *Energies*, Vol. 6, pp. 5538–5551, 2013.

[45] Z. Boudjema, R. Taleb, A. Yahdouand H. Kahla, "High order sliding mode control of a DFIM supplied by two power inverters," *Carpathian Journal of Electronic and Computer Engineering*, Vol. 8, No. 1, 2015, pp. 23–30.

[46] B. Beltran, M. E. Benbouzid and T. Ahmed-Ali, "Second-order sliding mode control of a doubly fed induction generator driven wind turbine," *IEEE Transactions on Energy Conversion*, Vol. 27, No. 2, pp. 261–269, 2012.

[47] D. Boudana, L. Nezli, A. Telmcani, M. O. Mahmoudi and M. Tadjine, "Robust DTC based on adaptive fuzzy control of double star synchronous machine drive with fixed switching frequency," *Journal of Electrical Engineering*, Vol. 63, No. 3, pp. 133–143, 2012.

[48] A. Abbou and H. Mahmoudi, "Performance of a sensorless speed control for induction motor using DTFC strategy and intelligent techniques," *Journal of Electrical Systems*, Vol. 5, No. 3, pp. 64-81, 2009.

H. Benbouhenni was born in chlef, Algeria. He is a Ph.D. student in the Department of Electrical Engineering at the ENPO-MA, Oran, Algeria. He received the M.A. degree in Automatic and Informatique Industrial in 2017. His research activities include the application of robust control in the wind turbine power systems**.**

Z. Boudjema was born in Algeria in 1983. He is Teacher in University of Chlef, Algeria. He received the M.Sc. degree in Electrical Engineering from ENP of Oran, Algeria in 2010. He received the Ph.D. in Electrical Engineering from University of Sidi Belabes, Algeria 2015. His research activities include the study and application of robust control in the wind-solar power systems.

A. Belaidi, Professor at the National Polytechnic High School - Maurice Audin in Oran. He obtained his Ph.D. in Physics at the University Of East Anglia - UK in 1980. His current fields of interest are Nanotechnology, Robotics and Artificial Intelligence.